Reprinted from the *Soil Science Society of America Journal*
Volume 42, no. 6, November–December 1978
677 South Segoe Rd., Madison, WI 53711 USA

Laterally Confined Flow From a Point Source at the Surface of an Inhomogeneous Soil Column[1]

S. D. MERRILL, P. A. C. RAATS, AND C. DIRKSEN[2]

ABSTRACT

Solution of a linearized flow equation for steady, axisymmetric, laterally confined infiltration from a point source located at the soil surface is compared with pressure head patterns measured in an undisturbed column of sandy loam. The geometry approximates an array of trickle irrigation emitters. The hydraulic conductivity could be represented as an exponential function of both the pressure head and the depth in the column. This implies that steady, multidimensional flow in the column is described by a linear flow equation.

Measured and predicted distributions of pressure head agreed most closely at an application rate of 0.5 cm/day. Increase in the size of a saturated zone about the point source at application rates higher than 0.5 cm/day caused isolines of pressure head to be distorted from the predicted shape. Flow patterns for homogeneous and heterogeneous soil are compared.

Trickle irrigation systems are usually operated intermittently. Measured distributions of pressure heads under intermittent application were compared with steady infiltration patterns. A steady-flow solution will give an approximate prediction of intermittent pressure head patterns for continuously repeated application cycles over part of the flow region and during part of the time.

Additional Index Words: **water, infiltration, hydraulic conductivity, drip irrigation, trickle irrigation.**

Merrill, S. D., P. A. C. Raats, and C. Dirksen. 1978. Laterally confined flow from a point source at the surface of an inhomogeneous soil column. Soil Sci. Soc. Am. J. 42:851–857.

DRIP AND TRICKLE irrigation has become important in the production of many tree and vegetable crops. Drip irrigation systems usually are operated intermittently and consist of a series of point or line sources, which are usually arrayed and interacting. Salts in the irrigation water can build up between the sources. For more effective design and use of drip systems, we need to be able to predict water movement from interacting sources.

Thus far, analytical solutions to equations describing unsteady, multidimensional flow in unsaturated soil have been found only when restrictive assumptions are imposed. For example, if the hydraulic conductivity is an exponential function of the pressure head and a linear function of the water content, then the equation for time-dependent, multidimensional flow is linearized, readily yielding solutions (e.g., Warrick, 1974). Numerical solutions are technically complex, and often considerably less convenient to use than analytical solutions.

If a drip irrigation system is operated frequently, and water application periods are sufficiently long, the flow at some distance from the source approaches steady state. For steady flows, the exponential relationship between the hydraulic conductivity and the pressure head suffice to linearize the flow equation (Gardner, 1958; Raats, 1970). With increasing irrigation frequency, the range of water contents in the soil narrows (Rawlins and Raats, 1975) and the exponential conductivity relationship becomes more applicable.

Specific solutions of the linearized, multidimensional, steady flow equation have been described by a number of workers. Philip (1968, 1972) and Raats (1971, 1972) gave solutions for flow from isolated point sources and cavities at arbitrary depth. Solutions for isolated line sources were discussed by Philip (1971, 1972). Raats (1970) gave solutions for an array of line sources at the soil surface. Zachman and Thomas (1973) discussed laterally confined flows from line sources at arbitrary depth. The latter geometry was also used in experimental studies by Thomas et al. (1974) without plants and by Thomas et al. (1977) with plants. Dirksen (1978) described steady and transient water content distibutions around buried, interacting line sources and compared them with theoretical distributions for steady sources.

Raats (1977) gave a comprehensive set of solutions for laterally confined flows from point and line sources and to point and line sinks. The solution for axisymmetric, laterally confined flow from a point source at the soil surface is described in this paper. This type of axisymmetric flow approximates a square or hexagonal array of drip irrigation sources. An exact solution for flow from an array of point sources is approached by summation of a large number of solutions for isolated point sources, but this is awkward in derivation.

The main objective of this study was to compare observed pressure head distributions under steady infiltration from a point source with the pattern predicted by theory. Measurements were made in a large undisturbed soil column, which was found to be inhomogeneous. The theory cited here assumes homogeneous, isotropic soils exhibiting no hysteresis. Hence, a second objective was to examine the influence of hydraulic conductivity variation over soil depth upon flow pattern.

As the frequency of intermittent applications at a point source increases, flow approximately will become constant at shallower depths. If the amount of water applied during each cycle is the same, steady flow is approached or approximated during part of the application cycle. In view of this, a third objective of the study was to compare pressure head distributions under repeated, intermittent water application with those established by continuous application.

THEORY

For steady flow, in the absence of uptake by plant roots, the balance of mass may be stated as

[1]Contribution from the U. S. Salinity Laboratory, Science and Education Administration, USDA, 4500 Glenwood Dr., Riverside, CA 92501. Received 6 Mar. 1978 Approved 26 June 1978.

[2]Formerly Physicist and formerly Soil Scientists. Current location of S. D. Merrill is Northern Great Plains Research Center, USDA-SEA, P. O. Box 459, Mandan, ND 58554; current location of P.A.C. Raats is Instituut voor Bodemvruchtbaarheid, Oosterweg 92, Haren (Gr.), The Netherlands; current location of C. Dirksen is Laboratory of Soils and Fertilizers, Agricultural State Univ. Wageningen, The Netherlands.

$$\nabla \cdot f = 0, \quad [1]$$

where f is the volumetric flux vector and ∇ is the vector differential operator. The flux is assumed to be adequately described by Darcy's law

$$f = -k\nabla h + k\nabla z, \quad [2]$$

where h is the pressure head, k is the hydraulic conductivity, and z, the depth, is positive downward. The total head is $H = h - z$. Combining [1] and [2] gives the basic equation for steady flow

$$-\nabla \cdot (k\nabla h) + \partial k/\partial z = 0. \quad [3]$$

Introducing the matrix flux potential,

$$\varphi = \int_{-\infty}^{h} kdh = \int_{0}^{\theta} Dd\theta, \quad [4]$$

and the exponential dependence of k upon pressure head,

$$k = k_0 \exp(\alpha h), \quad [5]$$

yields a linearized flow equation in φ (Gardner, 1958; Raats, 1970),

$$-\nabla^2\varphi + \alpha\, \partial\varphi/\partial z = 0. \quad [6]$$

In equations here, θ is volumetric water content, k_0 is saturated hydraulic conductivity, and α is a proportionality constant. Equation [5] implies that the soil is isotropic and homogeneous.

Philip (1972) has shown that the form

$$k = k_0 \exp[\alpha(h + \beta z)],\ \beta \geq 0 \quad [7]$$

is mathematically convenient for exploring flow in isotropic yet inhomogeneous, soil where hydraulic conductivity increases or decreases with depth. (The symbol β represents another constant.) As in Eq. [5], the relation

$$\varphi = \alpha^{-1} k \quad [8]$$

also holds for Eq. [7] if the integration in Eq. [4] is performed at constant z. The gradient of the matric flux potential for Eq. [7] is:

$$\nabla\varphi = k(\partial h/\partial x)\ j_x + k\,(\partial h/\partial y)\ j_y + [k(\partial h/\partial z) + k\beta]\ j_z, \quad [9]$$

where the j_i are unit vectors, and the flow equation in φ becomes

$$-\nabla^2\varphi + \alpha(1 + \beta)\, \partial\varphi/\partial z = 0. \quad [10]$$

For homogeneous soil, $\beta = 0$, and any solution of Eq. [10] reduces to a solution of Eq. [6] by setting the value of β equal to zero. For buried or surface-located sources, β must be ≥ 0 for solutions to be consistent with the exponential conductivity relationship, Eq. [7], which is appropriate only for unsaturated soil, where $h \leq 0$ (see Philip, 1972, and Philip and Forrester, 1975).

We are interested in the solution of Eq. [10] for the geometry shown in Fig. 1A. For axisymmetric flow the appropriate dimensionless version of Eq. [10] is (Raats, 1977, Eq. [74]):

$$\frac{\partial^2\Phi}{\partial R^2} + \frac{1}{R}\frac{\partial\Phi}{\partial R} + \frac{\partial^2\Phi}{\partial Z^2} = \alpha(1 + \beta)\mathcal{R}\,\frac{\partial\Phi}{\partial z}, \quad [11]$$

where the dimensionless radial and vertical coordinates are defined as

$$R = r/\mathcal{R} \text{ and } Z = z/\mathcal{R}, \quad [12]$$

and the dimensionless matric flux potential is

$$\Phi = (\pi\mathcal{R}/S)\varphi. \quad [13]$$

S is the source strength (volume/time), and $\mathcal{R}$ is the actual radius of the cylindrical flow region. Upper case letters represent dimensionless quantities, lower case, dimensional. An equation analogous to [11], written in terms of the dimensionless Strokes stream function,

$$\Psi = (1/S)\psi, \quad [14]$$

is (see Raats, 1977, Eq. [77]):

$$\frac{\partial^2\Psi}{\partial R^2} - \frac{1}{R}\frac{\partial\Psi}{\partial R} + \frac{\partial^2\Psi}{\partial Z^2} = \alpha(1 + \beta)\mathcal{R}\frac{\partial\Psi}{\partial Z}. \quad [15]$$

For this study we are interested in the particular solutions of Eq. [11] and [15] for a laterally confined, surface point source, with boundary conditions indicated in Fig. 1A. Raats (1970, 1977) pointed out that the boundary conditions for laterally confined flows, are such that it is most convenient to solve the problem in terms of the dimensionless stream function, Ψ, and then to obtain the expression for Φ from an analog of the Cauchy-Rieman conditions. Raats (1977) gives expressions for point sources at a distance Z_0 below the soil surface. We are interested in the expressions resulting from taking the limit $Z_0 \to 0$ of solutions for $Z > 0$ and substituting $\alpha(1 + \beta)$ for α (see Eq. [84], [90], [92], [93], and [96], Raats, 1977). The resulting dimensionless stream function (Ψ), matric flux potential (Φ), and radial (F_r) and vertical (F_z) components of the flux are, respectively:

$$\Psi = R^2 + \Sigma\{2/[\lambda_n J_2^2(\lambda_n)]\} \exp(-P_n{}^+ Z) R J_1(\lambda_n R), \quad [16]$$

$$\Phi = [\alpha(1 + \beta)\mathcal{R}]^{-1} + \Sigma\{P_n{}^+/[\lambda_n{}^2 J_2^2(\lambda_n)]\} \exp(-P_n{}^+ Z) J_0(\lambda_n R), \quad [17]$$

$$F_r = \Sigma\{P_n{}^+/[\lambda_n J_2^2(\lambda_n)]\} \exp(-P_n{}^+ Z) J_1(\lambda_n R), \quad [18]$$

$$F_z = 1 + \Sigma\{1/J_2^2(\lambda_n)\} \exp(-P_n{}^+ Z) R J_0(\lambda_n R). \quad [19]$$

The summations here are from 1 to ∞ and $P_n{}^+$ is given by:

$$P_n{}^+ = -[\alpha(1 + \beta)\mathcal{R}/2]^2 + \{[\alpha(1 + \beta)\mathcal{R}/2]^2 + \lambda_n{}^2\}^{1/2} \quad [20]$$

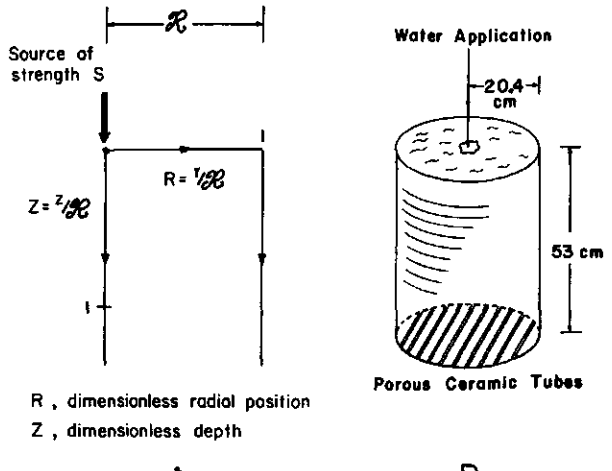

Fig. 1—*(A)* Diagram of the flow region studied with the boundary conditions for Ψ. *(B)* diagram of the cylindrical, soil column used for the measurements.

J_0, J_1, and J_2 are Bessel functions, and the λ's are the zeroes of J_1, i.e., $J_1(\lambda_n) = 0$. The first 40 λ's are given in Watson (1966, p. 748). Subsequent zeroes are spaced at intervals of approximately π.

The use of dimensionless variables and the exponential dependence of conductivity result in solutions depending only on $\alpha(1 + \beta)\mathcal{R}$ (or $\alpha\mathcal{R}$ in the case of homogeneous soil). This illustrates the advantages of using the exponential conductivity relations [5] and [7].

In numerical calculations, one may convert dimensionless matric flux potential to pressure head by use of

$$h = (1/\alpha)\ \ln[\Phi S\alpha)/(\pi\mathcal{R}k_0)] - \beta\mathcal{R}Z, \qquad [21]$$

which is derived by combining [7], [8], [12], and [13]. Equation [21] shows that, given α, β, k_0, $\mathcal{R}$ and S, there is a one-to-one relation between h and Φ, and since $\varphi = \alpha^{-1}k$, between h and k. Equation [21] also shows that if $\beta > 0$, the dimensionless depth, Z, enters the $h - \Phi$ and $h - k$ relations as a linear term in Z.

Measurements

An undisturbed, cylindrical soil sample of dimensions indicated in Fig. 1B was obtained by pressing a galvanized steel cylinder fitted with a cutting edge into the earth. Ten to fifteen cm of very loose material at the surface was removed. This soil is classified as Pachappa fine sandy loam (mixed, thermic, coarse loamy, mollic Haploxeralf). Drainage was provided by seating the cylinder upon a base containing ceramic tubes, each of which had an outside diameter of 1.2 cm. Loessal soil was packed around the tubes, which were placed 2 cm from center to center. Tensiometers were located at depths of 3.5, 7, 14, 28, and 42 cm and at radial positions 0, 6, 12, and 18 cm from the center of the cylinder. Two sets of tensiometers with 20 in each set, were installed in the soil cylinder. The horizontally placed shafts of the tensiometers were 6.5 mm in diam. and ended in highly porous ceramic tubes 12 to 15 mm long and 5 mm in outside diameter. (filter elements, Selas Corp., Springhouse, Pennsylvania).[3]

Water was applied through a small, glass tube at the center of the soil surface. A peristaltic pump was used to precisely control the flow through the emitter. During steady applications, pressure heads were measured by either water or mercury manometers. During intermittent applications, pressure heads were automatically recorded from a sensitive differential pressure transducer (Sandstrand Data Control, Inc.) by sequentially connecting the tensiometers to the sensor with a rotary, hydraulic valve.

At sufficient depth under steady infiltration from the point source, pressure head will become constant with depth in an arbitrarily deep soil profile. To simulate this condition to the extent possible, the vacuum level on the drainage ceramics was adjusted to obtain approximately the same pressure heads at the 42- and 52-cm depths.

Hydraulic conductivities were measured under steady and approximately unidirectional flow from seven emitters placed in an hexagonal array at the surface of the soil cylinder. The seven emitters were identical to the single emitter used for study of axisymmetric flows in the cylinder, and were also controlled with a peristaltic pump. The emitters were positioned so that each was 13.7 cm from neighboring emitters and 6.8 cm from the edge of the cylinder. During hydraulic conductivity measurements, the soil water content was changed monotonically along principal wetting and drying curves, ascending from a pressure head of approximately −350 cm water to the approximate bubbling pressure of about −20 cm water, and then descending.

[3]Company names are included for the benefit of the reader and mention does not imply any endorsement or preferential treatment of the product listed by the U. S. Department of Agriculture.

RESULTS AND DISCUSSION

Steady Infiltration

Hydraulic conductivities for four depth zones in the undisturbed soil core are shown in Fig. 2A. Although only four flow rates were used, the resulting pressure head values were distributed over the range encountered during the measurements of flow patterns from a single emitter (point source). Adherence to an exponential relation between hydraulic conductivity and pressure head is evident for both wetting and drying sequences of measurements. Rijtema (1965) showed plots of hydraulic conductivity vs. pressure head for a variety of soil types that adhere to the exponential relationship.

The slopes, α, of the hydraulic conductivity curves in Fig. 2A show no consistent relationship with depth and no significant difference between wetting and drying sequences of measurements. The absolute value of the

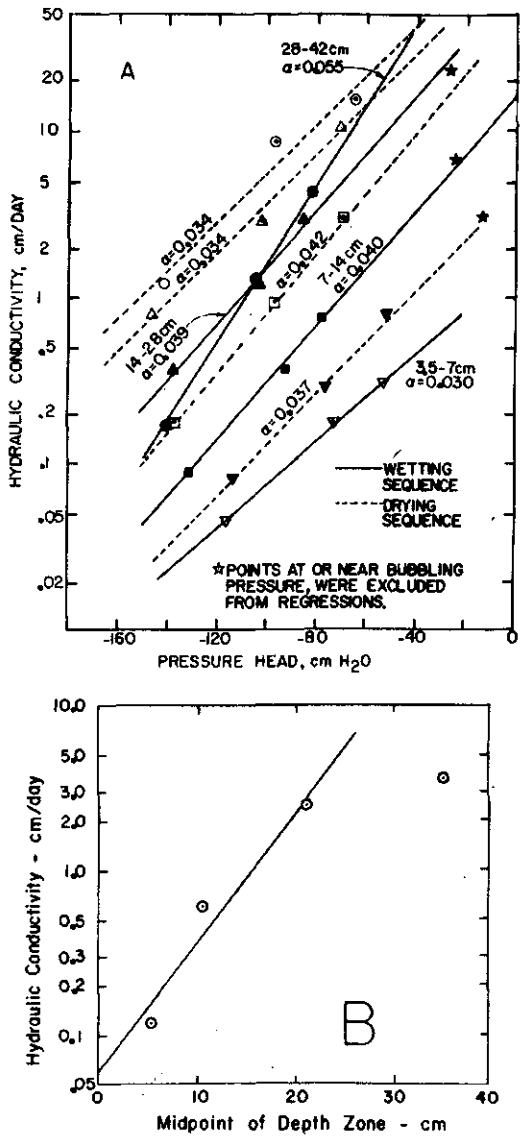

Fig. 2—*(A)* Hydraulic conductivity as a function of the pressure head in various layers for wetting and drying sequences of measurements. *(B)* hydraulic conductivity at a pressure head of −95 cm of water as a function of depth.

hydraulic conductivity does vary greatly with depth. Figure 2B shows the hydraulic conductivity at a pressure head of −95 cm water as a function of depth. As the slopes of the log hydraulic conductivity vs. pressure head curves (the α values) fall within a narrow range of values, the slopes of log hydraulic conductivity vs. depth curves (the β values) at different pressure heads will also fall within a restricted range of values. The hydraulic conductivity for each layer was taken from a linear regression equation for both wetting- and drying-sequences of measurements. The data show an exponential relationship between hydraulic conductivity and the midpoint depths of the upper three zones, but not of all four zones. Using an average value for α of 0.0369 cm^{-1}, the value of β (see Eq. [7]) extracted from the data in Fig. 2A is 4.98 (dimensionless). The parameter k_0 was found to be 1.945 cm/day. Here we have an example of a natural soil profile showing approximate exponential increase in hydraulic conductivity with depth over at least part of the profile.

To make the comparisons between measured and predicted pressure head patterns we have measured hydraulic conductivity over depth zones 3.5, 7, or 14 cm thick, as set by tensiometer placement. Conductivity measurements even more precisely localized in depth would have been desirable. A sorptivity technique explored by Dirksen (1975) enables one to conveniently and rapidly make in situ hydraulic conductivity measurements that are localized within a depth of 1 or 2 cm below a ceramic disk. This technique allows conductivity inhomogeneities to be directly examined in the field. Tensiometer techniques, such as the one used in this study, do not appear to be as practical as the sorptivity method for finer scale examination of hydraulic conductivity inhomogeneities.

Pressure head patterns measured at four different steady-flow rates are displayed in the upper part of Fig. 3. The wetting-drying history leading to the times when these patterns were recorded was complex, and no effort was made to control this as was done for the hydraulic conductivity measurements. As the flow rate increases, the pressure head isolines show greater horizontal spreading. This is due to ponding of water at the soil surface around the source and nearly saturated conditions immediately below it. At an application rate of 2 cm/day, free water was visible over a radius of 4.5 cm; at an application of 1 cm/day, the pond would shrink to approximately a 3-cm radius.

The values of α, β, and k_0 given above were used in equations [17] and [21]. The resulting pressure head patterns are shown in the bottom part of Fig. 3. In these theoretical patterns, there is no change in the shapes of the isolines because of horizontal spreading as the rate of application increases. According to the theory, pressure heads and corresponding hydraulic conductivities increase without limit as the point source is approached.

In the measured patterns, there is very little gradient in pressure head below the dimensionless depth $Z = 0.7$ (14 cm dimensional), whereas the theoretical patterns show an increasingly uniform and finite pressure head gradient with increasing depth. This is due to the apparently more uniform hydraulic conductivity below $Z = 0.7$ in the soil. Note that the hydraulic conductivities of the 14- to 28-cm and the 28- to 42-cm depth zones (see Fig. 2B), taken

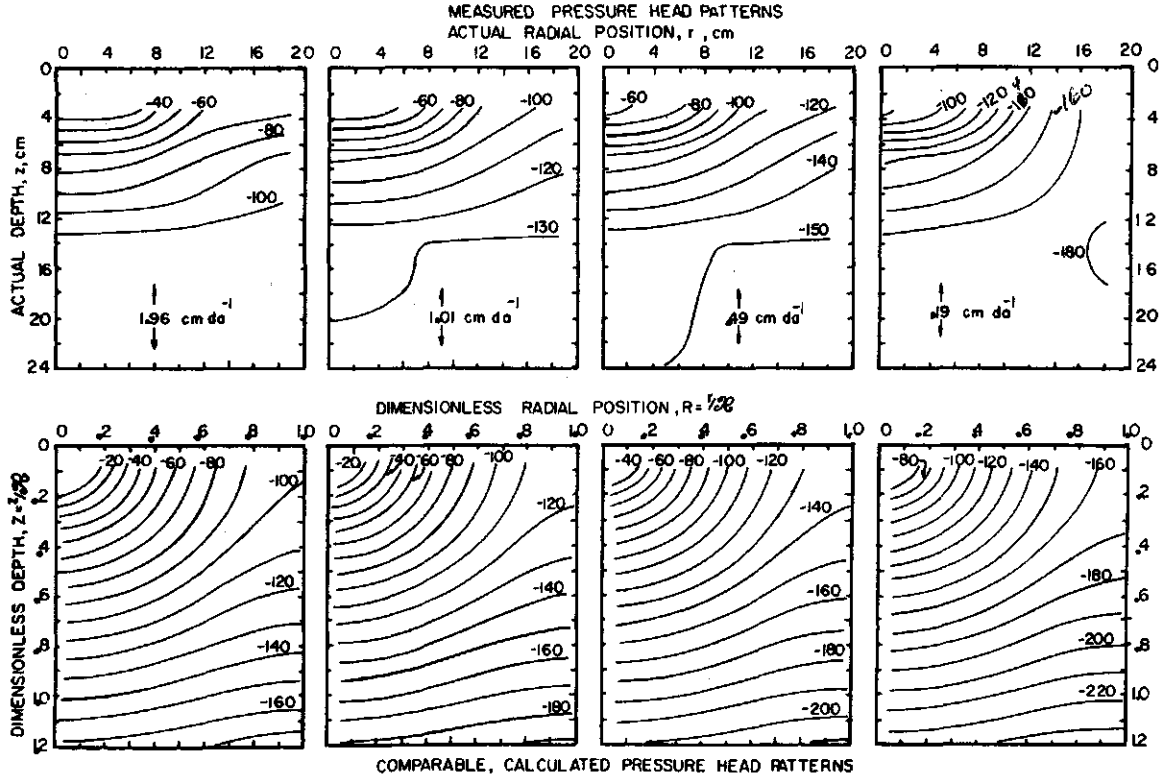

Fig. 3—Upper row: measured distribution of pressure head for various steady infiltration rates from a point source; Lower row: distribution of pressure head calculated on the basis of parameters given in text for same four application rates.

together, do not follow the exponential increase of conductivity with depth.

For a given value of $\alpha\mathcal{R}$ or of its equivalent, $\alpha(1+\beta)\mathcal{R}$ in inhomogeneous soil, there is only one solution in Φ for the boundary conditions used here. Also, for a given set of values of α, β, k_0, and $\mathcal{R}$, the value of h at any given point, (R, Z), at a given application rate, S_1, will differ from the h value at (R, Z) under another application rate, S_2, by the constant $\ln(S_1/S_2)/\alpha$. This is shown by rearrangement of Eq. [21]:

$$h - (\ln S)/\alpha = \alpha^{-1}\ln(\Phi\alpha/\pi\mathcal{R}k_0) - \beta\mathcal{R}Z \quad [22]$$

For a given set of specifying parameters, other than S, and at a given point, (R, Z), the righthand side of [22] is constant. Theoretically coincident isolines of measured pressure heads at four different flow rates are graphed for two levels of $h - (\ln S)/\alpha$ in Fig. 4, along with the calculated isolines at a flow rate of 1.01 cm/day. The lines for each group should coincide for perfect agreement between theory and experiment. Again, the effect of surface ponding is apparent. However, the differences between positions of measured and calculated isolines at various flow rates are generally no more than 4 cm. This demonstrates the utility of the theory for at least semi-quantitative prediction of pressure head pattern around a point source steadily flowing without significant ponding.

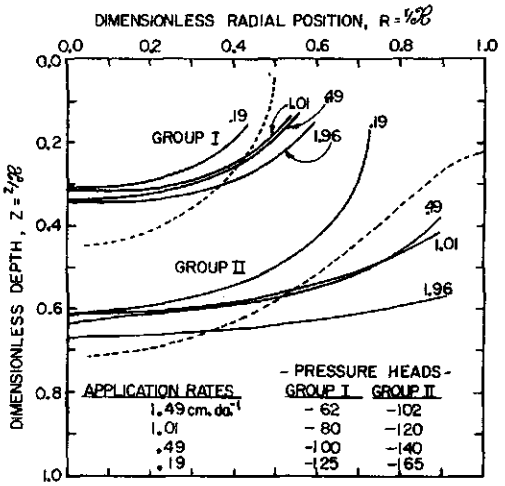

Fig. 4—Two groups of theoretically coincident pressure head isolines for the same four steady application rates as shown in Fig. 3, upper row. The solid lines are from measured data; the dashed lines are calculated from theory.

Homogeneous vs. Inhomogeneous Soils

Equations [11] and [15] indicate that, for a given value of $\alpha(1+\beta)\mathcal{R}$, the theoretical Ψ and Φ distributions serve for all sets of values of the parameters α, β, k_0 and S, consistent with that value. Differences among various cases shows up only in the actual pressure head distributions. The differences between the theoretical pressure head patterns in homogeneous soil ($\beta = 0$) and those found in the inhomogeneous soil column, with $\beta = 4.97$, can be seen by comparing Fig. 5A with Fig. 3, bottom half. The pressure head pattern in Fig. 5A was calculated for $S = 1.01$ cm/day, $\mathcal{R} = 20.1$ cm, and a hydraulic conductivity approximately equal to that found in the 7- to 14-cm depth zone (k_0

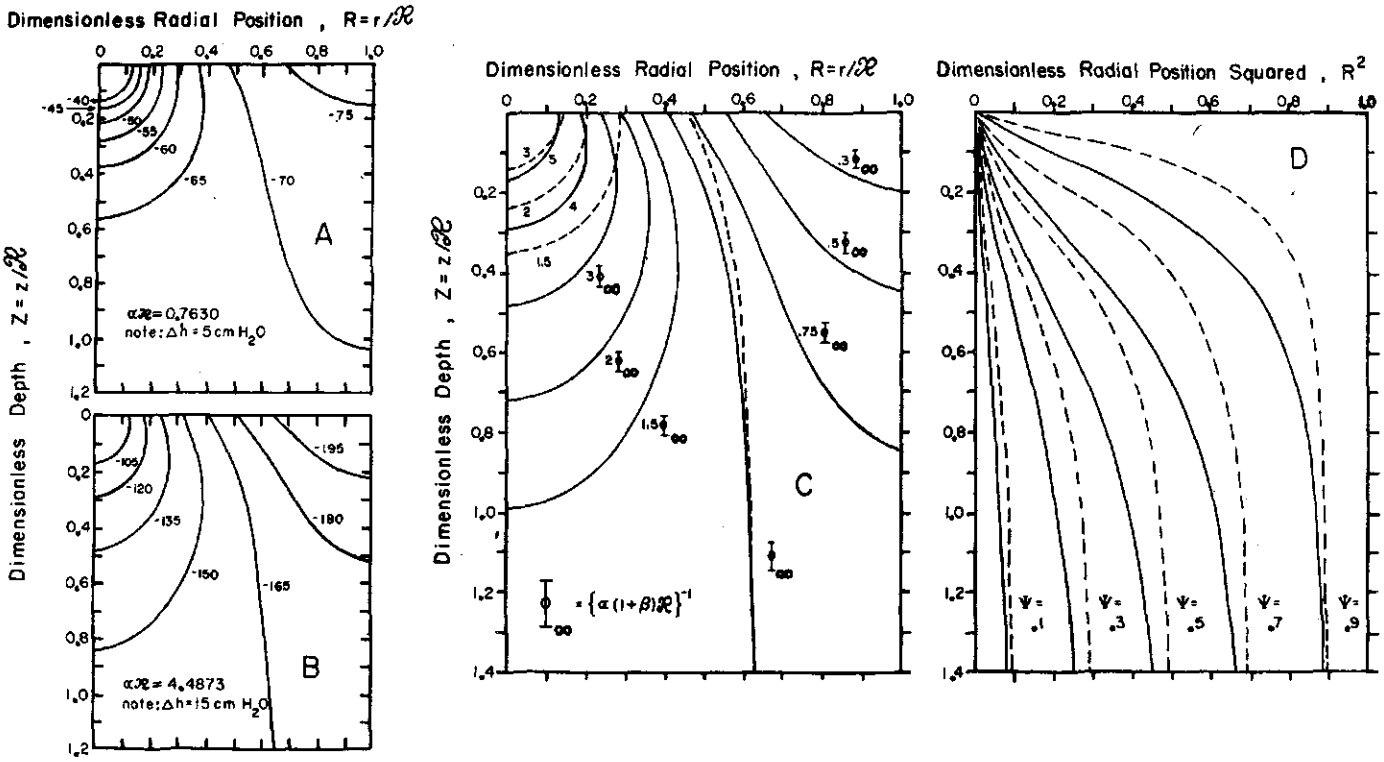

Fig. 5—(A) and (B) Calculated distribution of pressure head for steady infiltration from a point source at a rate of 1.01 cm/day in homogeneous soil ($\beta = 0$). The radius, $\mathcal{R}$, is 20.4 and 120.0 cm for A. and B., respectively, while $\alpha = 0.0374$ cm^{-1} for both. (C) Isolines of dimensionless matric flux potential calculated for $\alpha(1+\beta)\mathcal{R} = 0.763$, dashed isolines and $\alpha 1+\beta)\mathcal{R} = 4.487$, solid isolines. (D) Isolines of dimensionless stream function; dashed and solid isolines calculated for the same values of $\alpha(1+\beta)\mathcal{R}$ as in C.

= 1.95 cm/day with $\alpha\mathcal{R} = 0.763$). With β set equal to zero, Fig. 5A represents the h-distribution in a homogeneous soil. It can be seen in Fig. 5A that pressure heads are lowest in the upper corner of the flow region, whereas in the inhomogeneous soil (Fig. 3, bottom half) the pressure head becomes continuously lower with increasing depth. Philip and Forrester (1972) present an interesting series of figures showing the effect of β on h-distribution for laterally unconfined sources.

Thus, an increase in β from zero induces a considerable qualitative change in h-distribution. In contrast, if β is held constant, but pressure head patterns for different values of $\alpha\mathcal{R}$ are compared, less drastic, qualitative changes are induced. These changes are shown by comparison of Fig. 5A ($\alpha\mathcal{R} = 0.763$) with Fig. 5B ($\alpha\mathcal{R} = 4.487$), where $\beta = 0$ for both cases. Note that the latter value of $\alpha\mathcal{R}$ is numerically close to the value of $\alpha(1 + \beta)\mathcal{R}$ found in the actual, inhomogeneous soil. This adds another dimension of interest to the comparisons. The k_0 and S values are the same in Figs. 5A and 5B, but $\alpha\mathcal{R}$ is increased from 20.1 cm in Fig. 5A to 120.0 cm in Fig. 5B. The difference in isoline shapes between the two h-distributions shows the relatively greater influence of gravity in the Fig. 5B case—note the sagging of isolines—with its larger, actual flow region. If instead of the sixfold increase in $\mathcal{R}$ in Fig. 5B relative to Fig. 5A, a sixfold increase in α were introduced (resulting in the same $\alpha\mathcal{R}$ product), the h distributions would possess the same isoline shapes relative to the flow region, but the actual h values would differ from those shown in Fig. 5B. A greater value of α represents a coarsening of soil texture (see Rijtema, 1965, pp. 49, 50), which would also exert a greater gravitational influence on the h-distribution.

In constrast to the distribution of h, which is sensitive to both $\alpha(1 + \beta)\mathcal{R}$ and β, the distribution of the matrix flux potential, Φ, is sensitive only to the product $\alpha(1 + \beta)\mathcal{R}$. The same holds for the distribution of the hydraulic conductivity, k, which is a multiple of (dimensional) φ, as $\alpha^{-1}\varphi = k$ in this flow-equation linearization (see Eq. [8]). Fig. 5C presents dimensionless Φ-distributions for $\alpha(1 + \beta)\mathcal{R}$ values of 0.763 (dashed line) and 4.487 (solid line). Note that the isolines are in multiples of the Φ_∞ values for proper perspective (Φ_∞ is Φ at $Z \rightarrow \infty$). The solid line Φ-distribution in Fig. 5C shows difference from the dashed pattern analogous and qualitatively similar to the "gravitational sag" of the distribution of h shown in Fig. 5B.

Isolines of the dimensionless stream function, Ψ, if plotted over the flow region defined by Z and R^2, indicate the fraction of the cross-sectional area to which a given fraction of the total flow is confined as it diverges away from the point source and downward. Fig. 5D displays such a plotting of Ψ calculated for the two values of $\alpha(1 + \beta)\mathcal{R}$ (or $\alpha\mathcal{R}$) used for other parts of Fig. 5. The larger value of $\alpha(1 + \beta)\mathcal{R}$ (inhomogeneous case) results in a flow pattern more confined to the center of the region at a given depth. This has an important, practical implication: The type of inhomogeneity found in the undisturbed soil column, with hydraulic conductivity increasing with depth, will result in a more confined, maldistributed leaching of soil chemicals, nutrients, etc., than in comparable, homogeneous soil.

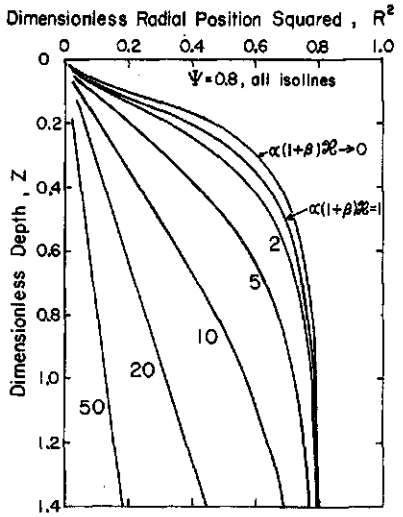

Fig. 6—Isolines of the dimensionless stream function at $\Psi = 0.8$ for several values of $\alpha(1 + \beta)\mathcal{R}$. Note that the abscissa is in R^2.

As $\alpha(1 + \beta)\mathcal{R}$ approaches zero, the equation for Φ reduces to Laplace's equation and the patterns of Φ and Ψ approach limiting forms. As $\alpha(1 + \beta)\mathcal{R}$ becomes greater, because of increasing $\mathcal{R}$, the streamline and potential patterns approach those of an isolated source. Of course, coordinate variables can no longer be scaled in $\mathcal{R}$ for isolated point and line sources, but in multiples of α (Raats, 1971; Philip, 1972). Figure 6 displays streamlines of Ψ for the axisymmetric flow studied here, for different values of $\alpha(1 + \beta)\mathcal{R}$. There is not much difference between the $\Psi = 0.8$ streamline when $\alpha(1 + \beta)\mathcal{R} = 1$ and when it approaches zero.

Steady vs. Intermittent Application

Drip irrigation systems are usually operated intermittently. Therefore, it is of interest to find out how closely steady flow theory can describe intermittent water application from a point source. Figure 7 shows the time course of pressure heads in the undisturbed soil column under an actual application rate of 2 cm/day, applied during alternating 6-hr on-off periods. Data presented in both Fig. 7 and 8 were collected after intermittent application programs were well established. Near the end of the 6-hr on-period, the pressure head values at the two greater radial distances from the source are approaching steady values, but pressure head traces at depths of 28 and 42 cm show quasi-sinusoidal variation. Figure 8 illustrates the approach to steady-application pressure head isolines for both 6- and 12-hr alternating on-off periods. For comparison, pressure head isolines under steady application at 1.96 cm/day and their theoretical equivalents are included in Fig. 8. Intermittent application isolines in all three parts of the figure show the effect of ponding near the source by the relative flatness of isoline slopes compared to the theoretical. Increasing flatness of the $h = -100$ cm isolines (middle of Fig. 8) apparently reflect accumulation of ponding with time. The intermittent and steady-flow measurements were made at different times, at slightly different temperatures, and undoubtedly under different wetting-drying history. All these factors had some adverse effects on the consistency

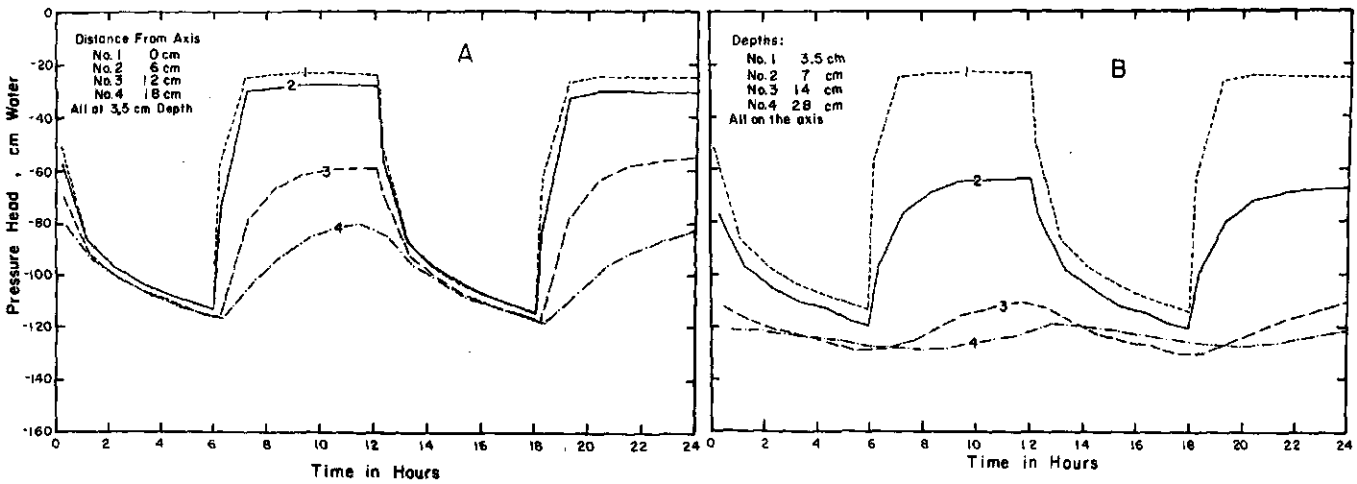

Fig. 7—Time-course of pressure heads measured under intermittent water application 6 hours out of every 12 at the point source: *(A)* At various distances from the column axis at a depth of 3.5 cm. *(B)* At various depths at the column center.

between steady- and intermittent-application isolines, as the measured $h = -60$ cm isoline under steady flow indicates.

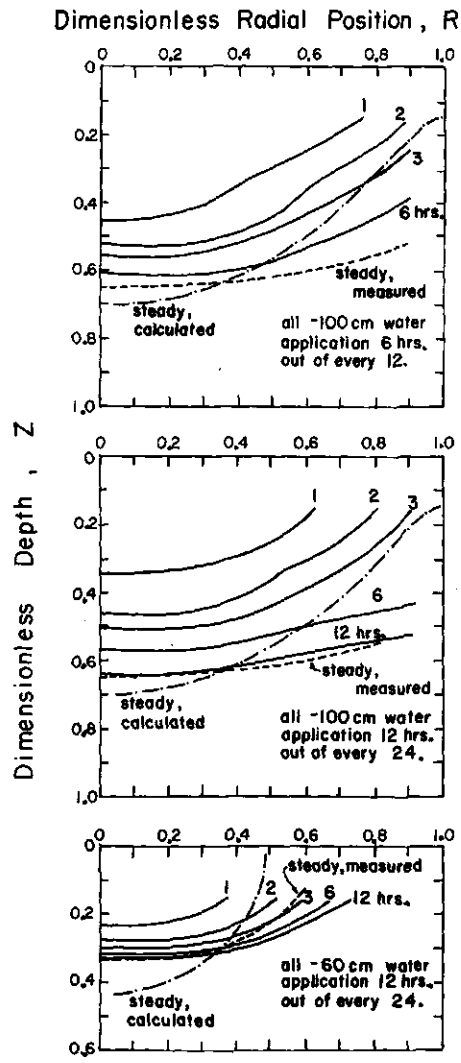

Fig. 8—Isolines of pressure head measured at various times after the start of application from the point source.

Acknowledgements

The authors thank Dr. A. W. Thomas for his useful comments on the manuscript.

LITERATURE CITED

1. Dirksen, C. 1975. Determination of soil water diffusivity by sorptivity measurements. Soil Sci. Soc. Am. Proc. 39:22–27.
2. Dirksen, C. 1978. Transient and steady flow from subsurface line sources at constant hydraulic head in anisotropic soil. Trans. ASAE Vol. 21, in press.
3. Gardner, W. R. 1958. Some steady-state solutions of the unsaturated moisture flow equation with application to evaporation from a water table. Soil Sci. 85:228–232.
4. Philip, J. R. 1968. Steady infiltration from buried point sources and spherical cavities. Water Resour. Res. 4:1039–1047.
5. Philip, J. R. 1971. General theorem on steady infiltration from surface sources with application to point and line sources. Soil Sci. Soc. Am. Proc. 35:867–871.
6. Philip, J. R. 1972. Steady infiltration from buried, surface, and perched point and line sources in heterogeneous soils. I. Analysis. Soil Sci. Soc. Am. Proc. 36:268–273.
7. Philip, J. R., and R. I. Forrester. 1975. Steady infiltration from buried, surface, and perched point and line sources in heterogeneous soils: II. Flow details and discussion. Soil Sci. Soc. Am. Proc. 39:408–414.
8. Raats, P. A. C. 1970. Steady infiltration from line sources and furrows. Soil Sci. Soc. Am. Proc. 34:709–714.
9. Raats, P. A. C. 1971. Steady infiltration from point sources, cavities, and basins. Soil Sci. Soc. Am. Proc. 35:689–694.
10. Raats, P. A. C. 1972. Steady infiltration from sources at arbitrary depth. Soil Sci. Soc. Am. Proc. 36:399–401.
11. Raats, P. A. C. 1977. Laterally confined, steady flows of water from sources and to sinks in unsaturated soils. Soil Sci. Soc. Am. J. 41:294–304.
12. Rawlins, S. L., and P. A. C. Raats. 1975. Prospects for high-frequency irrigation. Science 188:604–610.
13. Rijtema, P. E. 1965. Analysis of actual evapotranspiration. Center Agric. Pub. Documentation, Wageningen, The Netherlands, Agric. Res. Rep. No. 659.
14. Thomas, A. W., E. G. Kruse and H. R. Duke. 1974. Steady infiltration from line sources buried in soil. Trans. ASAE 17:125–128, 133.
15. Thomas, A. W., H. R. Duke, and E. G. Kruse. 1977. Capillary potential distributions in root zones using subsurface irrigation. Trans. ASAE 20:62–67, 75.
16. Warrick, A. W. 1974. Time-dependent linearized infiltration. I. Point sources. Soil Sci. Soc. Am. Proc. 38:383–386.
17. Watson, G. N. 1966. A treatise on the theory of Bessel functions. Univ. Press, Cambridge. 804 p.
18. Zachman, D. W., and A. W. Thomas. 1973. A mathematical investigation of steady infiltration from line sources. Soil Sci. Soc. Am. Proc. 37:495–500.